

H atom in elliptically polarized microwaves: Semiclassical versus quantum resonant dynamics

Krzysztof Sacha and Jakub Zakrzewski

Instytut Fizyki imienia Mariana Smoluchowskiego, Uniwersytet Jagielloński, ulica Reymonta 4, PL-30-059 Kraków, Poland

(Received 10 July 1998)

The dynamics of Rydberg states of atomic hydrogen illuminated by resonant elliptically polarized microwaves is investigated both semiclassically and quantum mechanically in a simplified two-dimensional model of an atom. Semiclassical predictions for quasienergies of the system are found to be in very good agreement with exact quantum data enabling a classification of possible types of motion and their dynamics with the change of the ellipticity of the microwaves. Particular attention is paid to the dynamics of the nonspreading wave packet states, which are found to exist for an arbitrary microwave polarization. [S1050-2947(98)07711-7]

PACS number(s): 05.45.+b, 32.80.Rm, 42.50.Hz

I. INTRODUCTION

Consider a hydrogen atom, initially in a high Rydberg state with the principal quantum number n_0 illuminated by the microwave field of a frequency ω close to the frequency of the unperturbed Kepler motion $\omega_K = 1/n_0^3$. Quantum mechanically speaking, a resonant periodic field couples strongly several n states due to almost resonant transitions $n \rightarrow n' = n \pm 1$ for n close to n_0 . Since the driving field is periodic, applying the Floquet theorem [1] one may find eigenstates of the atom-field system (the so-called Floquet or dressed [2] states). The eigenenergies are then referred to as quasienergies of the system and are defined modulo $\hbar\omega$. The Floquet states, periodic in time, may be viewed as linear combinations of unperturbed system eigenstates. While the construction of Floquet states is possible for both nonresonant and resonant driving, in the latter case they may have quite unusual properties, especially in a semiclassical limit.

Classically a resonance between the driving frequency and the frequency of the unperturbed motion leads to a strong perturbation of the system and a creation of a stable island in the phase space centered on a periodic orbit of the frequency ω . The motion in the island is locked to the microwave frequency due to the nonlinear resonance [3]. Semiclassically one then expects that the corresponding Floquet time-periodic state will follow a classical trajectory (in the vicinity of the periodic orbit), i.e., form a wave packet that will not disperse in time.

States localized in the resonance island for such a periodic perturbation have been first considered more than 20 years ago [4] and details of their semiclassical construction for some one-dimensional (1D) model systems have been analyzed [5,6]. The wave-packet character of the time evolution of individual Floquet states has been realized only quite recently [7] for a hydrogen atom driven by linearly polarized microwaves. Independently, it has been shown that Gaussian wave packets may propagate almost without dispersion along circular periodic orbits in hydrogen atoms driven by circularly polarized fields [8]. The fact that the harmonic approximation implied in [8] and resulting the Gaussian wave packet form is not a necessary condition for nonspreading properties have been discussed in [9,10] where it was shown that the harmonic expansion provides a good approximation for exact

Floquet states of the system (which by definition, being time periodic, do not spread on a long time scale).

The fact that one may construct in a nonlinear system wave packets that do not spread induced a flurry of activity in the field. Some [11–16] concentrated on modifying the potential so as to make the harmonic approximation as good as possible aiming at the construction of Gaussian nonspreading wave packets. Claiming that the anharmonic corrections are big for a hydrogen atom driven by circularly polarized fields those authors added a magnetic field perpendicular to the microwave polarization plane [11–16]. This helps to minimize the unharmonicities *in this plane*, leaving, however, unaffected the terms along the magnetic field axis. Thus the Gaussian wave packets still remain an approximation to the real dynamics and must disperse (although very slowly in time). Another approach aimed at optimizing the coordinate system to the symmetry of the problem is given in [17].

As discussed by us elsewhere [9,10,18–21] much more fruitful is another approach, already outlined above. Namely, we define the nonspreading wave packet as a single Floquet state (for which the Gaussian packet may be merely an approximation). Then a localization of the wave packet in the vicinity of a stable fixed point is assured by the correspondence principle provided the size of the surrounding island in the phase space is comparable to \hbar . One may construct an approximate resonance Hamiltonian in the vicinity of the island whose eigenstates will approximate well those Floquet states that are localized in the vicinity of the island (see below). Simultaneously, time periodicity of Floquet eigenstates assures that the exact Floquet states will not disperse.

The existence of such wave-packet Floquet eigenstates has been proven by an exact numerical diagonalization of the problem for both linear polarization (LP) [7] and circular polarization (CP) [9,10] of the microwaves. To allow their detection one should consider the ways of populating effectively such states. For a CP, where the direct optical excitation from a weakly perturbed low-lying state is impossible (since the wave packet is built from predominantly circular atomic states inaccessible from low-lying states due to dipole selection rules) one should first prepare the atomic circular state [22,23] and then switch on the microwaves sufficiently fast [9]. It has been shown that the wave-packet states may be populated in this way with about 90% efficiency

[24]. For a LP case, an addition of a static electric field allows one to control the trajectory of the wave packet [18], in particular wave packets moving along elongated, low angular momentum trajectories may be created. Such wave packets may be accessible to a direct excitation from low-lying states.

The next important question is the possible mechanism of the detection of these states. At least three possible ways suggest themselves. Two of them utilize the residual decay of wave packets, either via the spontaneous emission (treated both for LP [25] and CP [26,21]) or the ionization. The former may not be efficient, since, at least for wave packets moving on circular trajectories, the corresponding spontaneous emission rates are quite small [21]. In the ionization experiment, the population of the wave-packet state may be detected by a strong decrease in the ionization yield (since ionization rates of wave-packet states are typically very small [9,10]). On the other hand, these rates fluctuate strongly (the mechanism of their ionization, via ‘‘chaos assisted tunneling’’ is discussed in detail elsewhere [19,20])—this may make their detection in the ionization yield quite ambiguous.

By far the most promising method is the Floquet spectroscopy [27], i.e., probing, by a second weak microwave field, the structure of Floquet (dressed [2] by microwaves) states. To this end a precise estimation of the quasienergies of wave-packet states is necessary. An exact diagonalization of the problem gives all the Floquet states and a time consuming inspection of individual eigenvectors is necessary to identify the wave-packet states. This process may be optimized by calculating properties of matrix elements of appropriately chosen operators but certainly it is desirable to have good semiclassical predictions for the quasienergies. For the CP case those are given, to a very good accuracy from the harmonic approximation Hamiltonian [8–10], this approach being, however, restricted to this particular system.

For a general case of periodically driven systems there is no simple unitary transformation that removes the time dependence (as it is in the CP case) and the correct approach is to use approximate resonant Hamiltonians. The semiclassical quantization of such a Hamiltonian gives not only the good estimate for wave-packet states but allows for the classification of resonant states for systems of more than one dimension. Recently, using such an approach we could discuss the resonant dynamics in a realistic three-dimensional (3D) model of a hydrogen atom in the LP case [28]. Similarly, we have discussed the control of wave-packet trajectories using an additional static electric field [18].

Until now the discussion of nonspreading wave-packet states has been restricted to linear and circular polarization cases only. The aim of this paper is to treat a resonant dynamics of a hydrogen atom, both semiclassically and quantum mechanically in a general case of an elliptical polarization (EP). Apart from generalizing the notion of nonspreading wave packets to an arbitrary EP, we discuss the full dynamics of quasienergies as a function of the ellipticity of the microwaves for a resonant case, being stimulated by recent ionization experiments [29]. Unfortunately, the experiments do not allow for a full selection of the initial state of an atom (states with all possible angular momenta are

simultaneously excited) but this situation may improve in the near future.

The EP case is highly nontrivial. For LP microwaves the conservation of the angular momentum projection onto the polarization axis L_z makes the dynamics effectively two dimensional. For the CP case while L_z is not conserved, the transformation to the frame rotating with the microwave frequency removes the explicit oscillatory time dependence (see, e.g., [30–33]). Both these simplifications are no longer possible in the general EP microwave field. In effect, the exact quantum diagonalization approach for the part of the spectrum corresponding to the strongly perturbed atomic Rydberg spectrum would require very big computer memory. Let us mention also that in the effective 2D LP case, the state of the art computations [7] consider initial atomic states with the principal quantum number of the order of 20.

For that reason we shall consider not the realistic fully 3D model of an atom but rather the restricted 2D model in which the electronic motion is restricted to the polarization plane. Study of such simplified models has been most successful in the past both for LP (where one-dimensional model has been a main source of quantum results for a long time [34,35,6]) and in CP [30–33] where also the 2D, polarization plane restricted model has been utilized. An additional argument favoring the 2D model comes from our classical study of dynamics in EP microwaves [36,37] where comparison of 2D [36] and 3D [37] analysis shows the similarity of physical phenomena in both cases. Simply put the perturbation is most effective if the polarization plane coincides with the plane of Kepler motion.

II. SEMICLASSICAL VERSUS QUANTUM APPROACHES

The Hamiltonian of the hydrogen 2D model atom driven by an elliptically polarized electromagnetic field reads in the dipole approximation and in the length gauge (in atomic units)

$$H = \frac{p_x^2 + p_y^2}{2} - \frac{1}{r} + F(x \cos \omega t + \alpha y \sin \omega t), \quad (2.1)$$

where $r = \sqrt{x^2 + y^2}$ while F and ω denote the amplitude and the frequency of the microwave field, respectively. α defines the ellipticity of the microwaves with $\alpha=0$ ($\alpha=1$) corresponding to a LP (CP) limiting case.

Using the Floquet theorem the solution of the quantum problem is equivalent to diagonalizing the Floquet Hamiltonian

$$\left(H - i \frac{\partial}{\partial t} \right) \psi_n = H_F \psi_n = E_n \psi_n \quad (2.2)$$

with E_n being the quasienergies while ψ_n time-periodic Floquet eigenstates.

The details of the numerical method are described in the Appendix. In short, the calculations proceed by expressing the Floquet eigenvalue equation in the scaled semiparabolic variables

$$x = \Lambda \frac{u^2 - v^2}{2}, \quad y = \Lambda uv, \quad (2.3)$$

where Λ is an arbitrary scaling factor. This allows one to remove the Coulomb singularity and cast the Schrödinger equation into the generalized eigenvalue problem for polynomial-like operators. Standard harmonic oscillator creation and annihilation operators allow for simple evaluation of matrix elements. The approach closely resembles that for the 2D atom in the CP field [33] except that the explicit time dependence is treated by the Fourier expansion. It is worth stressing that using the complex scaling parameter Λ one effectively realizes the complex rotation in the system that enables the exact treatment of the coupling to the continuum (ionization); for details see [7,33] for LP and CP cases, respectively. In this paper, however, we shall concentrate on the Floquet level dynamics only for the sake of the comparison with the semiclassics. The analysis of the ionization phenomenon is left for a future publication.

The semiclassical quantization of resonant dynamics closely resembles the similar procedure applied by us recently for the LP case [18,28]. That in turn originates from a general prescription for EBK quantization of Floquet spectra [38].

Starting with the Hamiltonian (2.1) we remove the explicit time dependence by going to the extended phase space [3]. Defining the momentum p_t conjugate to t (time) variable we get the new Hamiltonian

$$\mathcal{H} = H + p_t, \quad (2.4)$$

which is conserved during the motion. The quasienergies of the system will be then the quantized values of \mathcal{H} .

As the next step we express the Hamiltonian in action-angle variables of the unperturbed Coulomb problem [36]. For the 2D model atom those are, e.g., the canonically conjugate pairs (J, θ) and (L, ϕ) . J is the principal action (corresponding to the principal quantum number, n_0). The corresponding angle θ determines the position of the electron on its elliptic trajectory. L is the angular momentum (equal to L_z for the 2D motion in the x - y plane) while ϕ is the conjugate angle (the angle between the Runge-Lenz vector and the x axis, i.e., the main axis of the polarization ellipse).

We shall consider below the case of the resonant driving, i.e., when the frequency of the Kepler motion $\omega_K = 1/J^3$ is close to the microwave driving frequency ω . Applying the secular perturbation theory [3] to average over the nonresonant terms one obtains an approximate resonant Hamiltonian (in the frame rotating together with the electron) of the form

$$\mathcal{H}_r = -\frac{1}{2J^2} - \omega J + F\Gamma(L, \phi; \alpha) \cos(\hat{\theta} - \delta) + \hat{p}_t, \quad (2.5)$$

where $\hat{\theta} = \theta - \omega t$ while $\hat{p}_t = p_t + \omega J$. \mathcal{H}_r yields the pendulumlike principal action motion with the strength and the equilibrium position determined by $\Gamma(L, \phi; \alpha)$ and $\delta = \delta(L, \phi; \alpha)$, respectively. The pendulum Hamiltonian is obtained by additionally expanding \mathcal{H}_r around the center of the resonance island given by $J = \omega^{-1/3}$ up to second order in $\Delta J = J - \omega^{-1/3}$ but we do not apply this expansion. Both Γ and δ depend on the initial shape and orientation of the electronic ellipse (via L, ϕ) as well as on the ellipticity of microwaves, α , and are given by [36,39]

$$\Gamma(L, \phi; \alpha) = \left[\left(\frac{1+\alpha}{2} V_1 \right)^2 + 2 \cos 2\phi \frac{1+\alpha}{2} V_1 \frac{1-\alpha}{2} V_{-1} + \left(\frac{1-\alpha}{2} V_{-1} \right)^2 \right]^{1/2}, \quad (2.6)$$

$$\tan \delta = \frac{(1-\alpha)V_{-1} - (1+\alpha)V_1}{(1-\alpha)V_{-1} + (1+\alpha)V_1} \tan \phi, \quad (2.7)$$

where

$$V_{\pm 1}(J, L) = \omega^{-2/3} \left[\mathcal{J}'_1(e) \pm \frac{\sqrt{1-e^2}}{e} \mathcal{J}_1(e) \right]. \quad (2.8)$$

$\mathcal{J}_1(x)$ and $\mathcal{J}'_1(x)$ denote the ordinary Bessel function and its derivative, respectively, while $e = \sqrt{1-L^2/J^2} = \sqrt{1-L^2\omega^{2/3}}$ stands for an eccentricity of an electronic ellipse. For completeness let us mention that a similar approximation on the purely quantum level, leading to Mathieu equation has been performed for the CP case only in [40].

The semiclassical quantization of Eq. (2.5) is straightforward and follows closely the procedure described in detail elsewhere [28] for arbitrary $m:1$ resonance. For 1:1 resonance considered here, the trivial quantization of \hat{p}_t , exploring the time periodicity of the system, yields additive terms $k\omega$ to quasienergies (different values of k correspond to different Floquet zones). As discussed first in [41], see also [28], the orbital motion in $(J, \hat{\theta})$ variables (along the perturbed Kepler ellipse) is much faster than the modification of the ellipse shape and its movement (precession) as described by the motion in (L, ϕ) . Thus the slow and fast motions may be adiabatically decoupled. Making Born-Oppenheimer approximation and using standard WKB rules, the fast $(J, \hat{\theta})$ motion is quantized taking the Maslov index $\nu=2$ (corresponding to librations, i.e., we quantize states inside the resonance island). Being interested in resonantly localized states we shall consider later the ground state of the radial motion, only. For the slow angular (L, ϕ) motion we take the Maslov index $\mu=0$ or 2 for a rotational or librational motion, respectively.

Similarly, as in the LP microwaves [28], it is easier to quantize first the slow motion generated by constant values of $\Gamma(L, \phi; \alpha)$ and later treat the fast motion. Such a procedure is justified since quantizing the fast motion one takes $\Gamma(L, \phi; \alpha)$ as a constant quantity and thus the order of the quantization does not matter.

The existence of the resonance island in $(J, \hat{\theta})$ space ensures that the radial motion is localized. So the remaining analysis should concern the angular (L, ϕ) motion, which reflects the slow evolution of the Kepler ellipse. The structure of the (L, ϕ) space influences values of quasienergies as well as the structure of corresponding semiclassical eigenstates. Trajectories in the (L, ϕ) space are determined by constant values of Γ also responsible for the size of the resonance island in $(J, \hat{\theta})$ space (recall that the island's size is determined approximately by $\sqrt{F\Gamma}$).

Before presenting the results let us define scaled variables, typically used as a convenient parametrization of the microwave ionization problem (since the dynamics scales

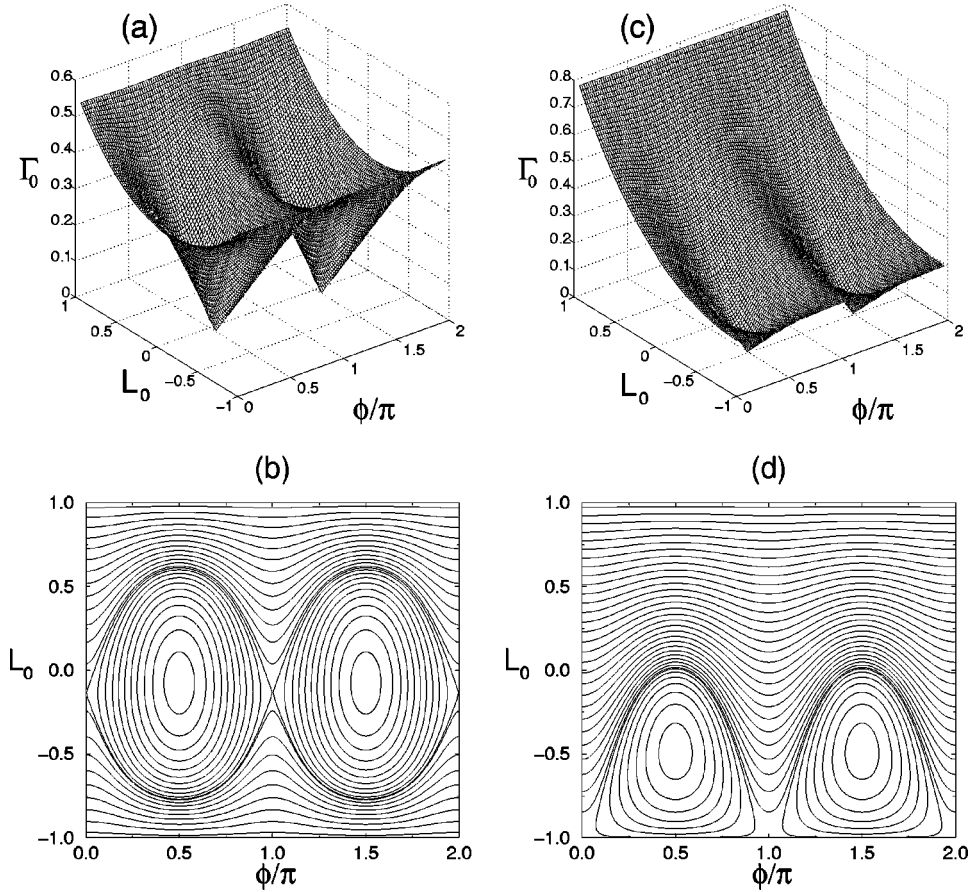


FIG. 1. Two-dimensional hydrogen atom illuminated by resonant, $\omega_0=1$, elliptically polarized microwaves. The effective scaled perturbation $\Gamma_0 = \Gamma/(n_0 + 1/2)^2$ is plotted as a function of the scaled angular momentum, L_0 , and the angle, ϕ , between the Runge-Lenz vector and the main axis of the polarization ellipse—upper row. Bottom row shows equipotential curves of the angular part Γ of the Hamiltonian \mathcal{H}_r , Eq. (2.5), representing the slow evolution of the Kepler ellipse. The curves correspond to semiclassical states originating from the $n_0=21$ hydrogenic manifold. Columns correspond to the different ellipticity of the microwaves $\alpha=0.1$ (left) and $\alpha=0.6$ (right).

classically [42]). The common choice is to link the scaling to the initial energy of the electron [35]. For an unperturbed 2D hydrogen atom the eigenenergies are given by $E_n = -1/2(n + 1/2)^2$ with n being non-negative integer. This allows us to define scaled variables via the principal quantum number of the initial state n_0 via

$$\omega_0 = \omega(n_0 + 1/2)^3, \quad (2.9)$$

$$F_0 = F(n_0 + 1/2)^4, \quad (2.10)$$

$$L_0 = L/(n_0 + 1/2). \quad (2.11)$$

In particular note that the scaled angular momentum L_0 may take values in the $[-1, 1]$ interval with extremal values corresponding to circular orbits on which the electron moves in two opposite directions.

III. RESULTS AND DISCUSSION

To compare the semiclassical predictions to the exact quantum calculations, we consider the $n_0=21$ manifold of our 2D model atom. This value is a compromise between the requirement to be in the semiclassical, large n_0 regime and computer memory limitations (size of the Floquet matrix to be diagonalized). For resonant driving we take the micro-

wave frequency to be $\omega = \omega_K = 1/(n_0 + 1/2)^3$, ($\omega_0 = 1$).

In Fig. 1 we present values of Γ as a function of the scaled angular momentum L_0 and the ϕ angle for two different values of the degree of the field ellipticity given by α . Equipotential curves of Γ corresponding to semiclassical states originating from $n_0=21$ hydrogenic manifold are also shown in the figure. Due to the specific form of the resonance Hamiltonian (2.5) those lines are *independent* of the microwave amplitude F .

For $\alpha=0$ the (L, ϕ) space is symmetric with respect to the $L_0=0$ axis since, in the LP case, dynamics is not affected by the direction of the rotation of an electron. The left column in Fig. 1 presents the results for $\alpha=0.1$, i.e., the case very close to the LP problem. Note the presence of four stable fixed points: two of them, $L_0 \approx 0$ and $\phi = \pi/2, 3\pi/2$, correspond to almost straight line orbits oriented perpendicularly to the main axis of the polarization ellipse, the other two fixed points correspond to circular orbits, $|L_0| \approx 1$ (for such orbits ϕ is a dummy variable), with an electron rotating in the same or opposite direction to the direction of the rotation of the field vector. In the vicinity of these fixed points the electronic motion is ‘‘shape’’ localized [since the motion remains in the vicinity of a given (L_0, ϕ) point the eccentricity of the orbit, $e = \sqrt{1 - L_0^2}$, as well as its orientation with respect to the polarization ellipse, given by ϕ is approxi-

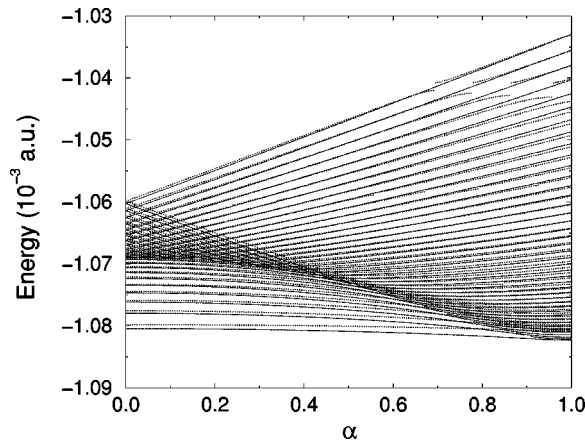


FIG. 2. Two-dimensional hydrogen atom driven by resonant, $\omega_0=1$, elliptically polarized microwaves. Level dynamics, vs α (i.e., the degree of the field ellipticity), of the semiclassical quasienergies (full lines) of the states originating from the $n_0=21$ hydrogenic manifold for $F_0=0.03$ compared with the exact quantum results (dotted lines).

mately preserved]. Whether the motion is well localized in its radial motion in $(J, \hat{\theta})$ variables, i.e., along the ellipse, depends on the size of the resonance island, given by $\sqrt{F\Gamma}$ as mentioned above. If the island in $(J, \hat{\theta})$ space is sufficiently large (comparable in size to \hbar or larger) the quantum state will be localized in the island. On the contrary, a too small resonance island cannot lead to localization in $(J, \hat{\theta})$ space, and possible quantum states will spread over the whole ellipse (then also the semiclassical approach used becomes obviously inadequate). Thus to observe interesting, nonspreading wave packets the resonance island must be large enough.

In this respect, two fixed points corresponding for small α to almost circular orbits, $|L_0| \approx 1$, lie at the maxima of Γ (compare the left top panel in the figure) and for sufficiently large F may enable a strong radial localization. The other two stable fixed points, corresponding to elongated orbits lie at local minima of Γ . There exist also two unstable fixed points around $L_0 \approx 0$ and $\phi = 0, \pi$; they form the origin of the separatrix dividing the space.

When α increases the fixed points situated initially around $L_0 \approx 0$ and $\phi = \pi/2, 3\pi/2$ move in the direction of greater negative values of L_0 (see the right column in Fig. 1), thus, the eccentricity of the corresponding orbits decreases. The circular orbits do not change the shape but the resonance island in $(J, \hat{\theta})$ space associated with $L_0 \approx 1$ becomes larger while that associated with $L_0 \approx -1$ becomes smaller as reflected by the greater and smaller values of Γ , respectively. Note also that the islands in the (L, ϕ) space containing librational states shrink with the increase of α , hence, they can support fewer and fewer semiclassical states—while α increases librational states vault over the separatrices and become rotational. In the limit of $\alpha=1$ the islands disappear and there exist only rotational states.

Consider the level dynamics corresponding to the change of α . Figure 2 shows the level dynamics for the group of states originating from the $n_0=21$ hydrogenic manifold. We take the scaled field amplitude $F_0=0.03$, which for the CP case corresponds already to a significant ionization yield [33] and may be, therefore, considered a quite large value. For the

LP case, i.e., $\alpha=0$, all states are doubly degenerate. Those of them that correspond to rotational states in the (L, ϕ) space are degenerate because the change of the rotation of an electron does not affect dynamics in the LP problem [the (L, ϕ) space is symmetric with respect to the $L_0=0$ axis]. The remaining librational states are degenerate as the two islands, around $L_0=0, \phi=\pi/2$ and $L_0=0, \phi=3\pi/2$, are identical and support identical states. Of course the degeneracies may be removed due to tunneling processes, for instance, the wave packets localized on circular orbits (the highest levels) rotate in the opposite directions and belong to distinct semiclassical states but quantum mechanical states are the symmetric or antisymmetric linear combination of them. Thus two wave packets propagating on a circular orbit in the opposite directions correspond to a single eigenstate (these wave packets were already discussed in [43] for the limiting LP case only). Similarly tunneling effects affect the librational states, i.e., quantum states are the linear combinations of solutions in each island.

An increase of α removes the semiclassical degeneracy of rotational states as one can see in Fig. 2—observe splittings of upper levels in the manifold. It corresponds to the broken symmetry with respect to change of a direction of rotation of an electron. Quasienergies of states corresponding to the motion in the opposite sense to the rotation of the field vectors, i.e., corresponding to negative values of L_0 , move down while those with positive L_0 go up. It is a consequence of the behavior of Γ , i.e., the greater Γ the greater the quasienergy value, see Fig. 1. Observe also that the degeneracy of all librational states (lower levels in Fig. 2) is not immediately removed after a slight change of the field ellipticity from $\alpha=0$ but is removed successively during an increase of α . This reflects the shrinking of the corresponding islands (the situation mentioned above), which causes the librational states to vault over the separatrix and become rotational. The levels with the smallest energy difference correspond to the librational and rotational orbits closest to the separatrix. The narrowing of the level spacing in their vicinity is just a consequence of the slowing down of the classical motion [44]. In the limit of $\alpha=1$ there is no degeneracy in the manifold.

Note that the energy splitting of the manifold is the largest in CP case while the smallest for LP. It is associated with the corresponding strength of the perturbation and simply expresses the dependence of Γ on α .

Exact quantum results coming from the numerical diagonalization of the Floquet Hamiltonian are presented also in Fig. 2. Among the multitude of Floquet states appearing in the same energy range only those with the largest overlap on the initial manifold are plotted for clarity. One can see that the agreement with the semiclassical predictions is very good except in the region of broad avoided crossings (with other levels—partners in the crossing eliminated by the overlap selection), which appear in the upper part of the figure. The semiclassical method does not take into account the interaction of the considered $n_0=21$ manifold with other manifolds (the method describes only a single resonant manifold), thus such avoided crossings have no chance to appear in our semiclassical calculations. For a more accurate comparison we plotted, in Fig. 3, quasienergies for two different values of α separately. The agreement between the semiclassical and quantum results is very good for high-lying levels

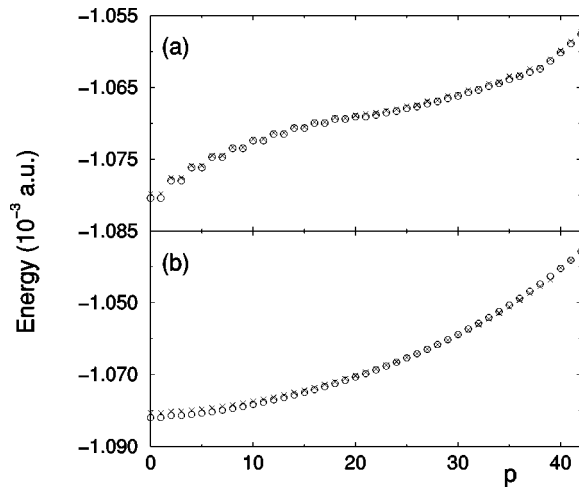


FIG. 3. Comparison of the semiclassical quasienergies (circles) originating from the unperturbed $n_0=21$ manifold for $F_0=0.03$ and $\omega_0=1$ with the exact quantum values (crosses), at different values of the degree of the field ellipticity $\alpha=0.1$ (a), 0.9 (b). Integer index p counts consecutive states in the perturbed manifold.

(greater values of Γ) while for lower levels some differences appear as expected due to small size of the resonance island.

In the limiting case $\alpha=1$, for the CP case, another analysis of resonant dynamics is possible, namely, a harmonic approximation around a stable equilibrium point in the rotating frame [8] (corresponding to the expansion about a stable fixed point $L_0=1$, ϕ arbitrary in our picture). It is interesting to compare both approaches. The present semiclassical quantization of the resonance Hamiltonian is certainly a more general approach valid for a general EP case and for the whole manifold. The harmonic expansion is limited to the CP case and valid for highest-lying states in the manifold only. On the other hand this expansion is quadratic in deviations from the equilibrium point but nonlinear in the microwave field F strength while the resonance Hamiltonian approach is a first order in F expansion. Clearly in the deep semiclassical regime (large n_0) and for sufficiently large F_0 the harmonic expansion approach yields a better approximation for wave packet states in the CP than the present resonant Hamiltonian analysis (yielding, however, little information on the energies of other states in the resonant manifold). On the other hand, quite surprisingly, we have found, by a direct comparison of numerical values, that for F_0 around 0.01 or 0.06 and n_0 up to 30 – 40 the resonant Hamiltonian yields semiclassical values closer to exact quantum data than the harmonic expansion. Thus for an intermediate range of n_0 and F_0 values the resonant Hamiltonian quantization is surprisingly good in accuracy, yielding, at the same time, the predictions for the whole resonant manifold and for an arbitrary polarization.

To complete the picture we show in Fig. 4 the level dynamics of the same $n_0=21$ manifold versus scaled field amplitude, F_0 , for $\alpha=0.6$. Quantum results are presented together with the semiclassical ones. Again, for the resonance island in orbital ($J, \hat{\theta}$) motion sufficiently large to capture quantum states, semiclassical results reproduce quantum ones quite well even beyond a classical chaos border (of course except avoided crossings).

Exact quantum Floquet matrix diagonalizations, per-

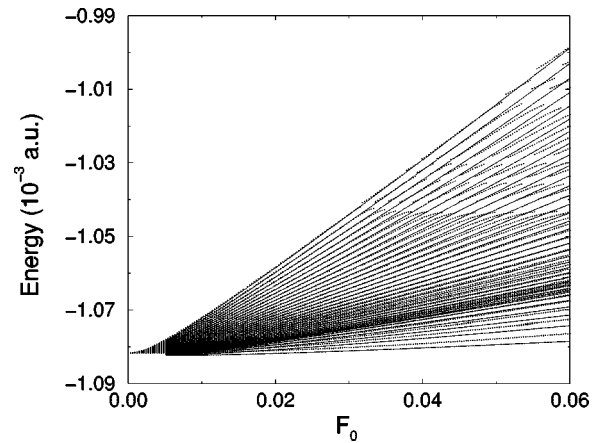


FIG. 4. Level dynamics of the exact quantum quasienergies (dotted lines) in the vicinity of the resonant manifold emerging from $n_0=21$, compared with the semiclassical prediction (full lines), for $F_0=0, \dots, 0.06$ and $\alpha=0.6$, $\omega_0=1$. Note that the maximum field amplitude clearly exceeds typical ionization thresholds measured in current experiments at the principal resonance. The semiclassical prediction accurately tracks the exact solution across a large number of avoided crossings.

formed using the Lanczos code yields not only the eigenvalues but also the corresponding eigenvectors. Their time evolution may be visualized [45] to confirm directly that indeed the Floquet states localized both in ($J, \hat{\theta}$) and in (L, ϕ) spaces correspond to the nonspreading localized wave packets. Consider again the level dynamics presented in Fig. 2. As discussed above the higher-lying state in the manifold corresponds to the wave-packet motion of the electron on the circular orbit in the direction coinciding with the direction of rotation of the electric field vector. And indeed such a motion is revealed by the plots of the corresponding Floquet state (see Fig. 5, upper row). This Floquet state changes little with change of the ellipticity of the microwaves, α , and in the limiting case of CP becomes a well-known CP nonspreading wave packet [8,9]. In the opposite limit of $\alpha=0$ i.e., the LP microwave case, this state becomes almost degenerate with another one corresponding to the different direction of the electron rotation. The two, almost degenerate exact Floquet states are linear combinations of the two wave packets (at least in 2D) as discussed in [43].

It seems interesting to see what happens to the second member of the pair as polarization is changed from linear to elliptical (α increases). The two states separate fast in α and each of them represents a distinct motion. As mentioned above the state going down in energy corresponds to a wave packet moving on the circular orbit in the direction opposite to the field. It undergoes a series of avoided crossings with other states of the manifold losing progressively its localized character. Still, for α not too large, and far from avoided crossings its wave-packet character is clearly visible (compare lower row in Fig. 5). This state loses its wave-packet character when the librational islands (compare Fig. 1) move sufficiently far down so that rotational states with large negative L_0 disappear since there is no “space left” for them due to the finite value of \hbar . As may be seen by comparison of Figs. 1 and 2 this transition occurs around $\alpha=0.45$ for $n_0=21$, manifesting itself in the quantum data (Fig. 2) by

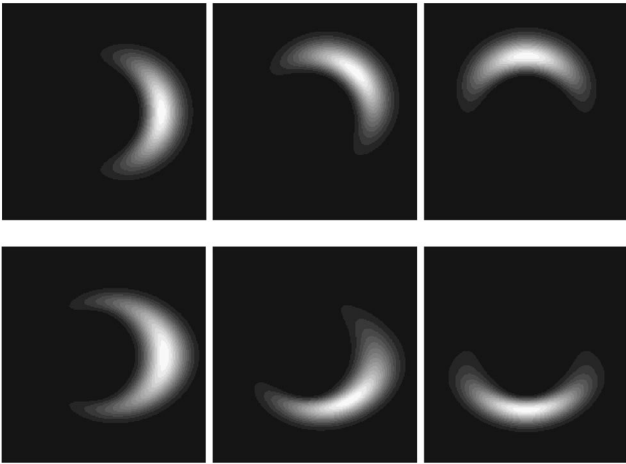


FIG. 5. Nonspreading wave packets for a 2D hydrogen atom illuminated by the elliptically polarized microwaves with the amplitude $F_0=0.03$, frequency $\omega_0=1$ for $n_0=21$ and ellipticity $\alpha=0.4$. Top row: the exact Floquet state corresponding to a nonspreading wave packet moving on a circular orbit in the direction of the rotation of the microwave field at times $\omega t=0, \pi/4, \pi/2$ from left to right. This wave packet corresponds to the one known for the circular polarization and may be obtained from the latter by a change of the microwave polarization. Bottom row: another exact Floquet state corresponding to a nonspreading wave packet moving in the opposite direction (shown at the same times $\omega t=0, \pi/4, \pi/2$ from left to right). Note that while the former almost preserves its shape in temporal evolution, the latter becomes significantly distorted. Still being an exact Floquet time-periodic eigenstate it regains its shape (as depicted, e.g., in the bottom left corner of the figure) every period of the microwave. The size of each box is ± 800 Bohr radii in both x and y directions.

relatively broad avoided crossings encountered by the wave-packet state. The transition point is, of course, \hbar dependent, for smaller \hbar (larger n_0) the rotational, wave-packet-like, state with large negative L_0 exists for larger α . It is worth stressing that for α below this critical, n_0 - (and thus driving frequency) dependent value there are two distinct Floquet states corresponding to two wave packets moving in opposite directions.

IV. CONCLUSIONS

To conclude we have shown, by comparison with the quantum numerical results, that the proposed semiclassical method, based on the first-order resonant Hamiltonian, gives good quantitative predictions. Numerical calculations produce nothing but numbers and an advantage of a semiclassical analysis is an understanding of what physics is hidden behind them. Apparently the behavior of the H atom placed in the EP microwave field, in the range of parameters used above, is determined by the underlying classical dynamics; especially, one may build wave packets that follow classical trajectories without spreading. We have shown that the wave packet discovered in CP microwaves [8,9] corresponding to the motion of the electron on a circular orbit in the same direction as the rotation of the microwave field exists also in EP case. For a sufficiently small ellipticity of the microwave polarization, α , there exists also another wave packet state,

corresponding to electron rotating in the opposite direction to the microwave field. In the limiting LP case both wave packets coalesce, the exact Floquet states correspond semiclassically to linear combinations of two wave packets propagating in the opposite direction on the circular orbit [43].

The analysis presented is restricted to the two-dimensional model atom (similar assumption is implicit in [43]), its validity for the real three-dimensional atom is an open question. Certainly, in the limiting LP case, due to rotational symmetry with respect to the field axis, the two wave packets moving in the opposite directions in 2D lead in 3D to a doughnut shaped localized function oscillating between north and south poles of the sphere (assuming a vertical polarization of LP microwaves) [28]. For CP, on the other hand, the wave-packet motion remains essentially two dimensional [10]. It will be most interesting to see how the third dimension affects the dynamics also for a general case of EP microwave field since already classical studies [36,37] indicate that some qualitative differences may appear. This subject is left for future studies.

Still the present 2D analysis shows that the nonspreading wave-packet states localized on circular orbits are not restricted to circular polarization of microwaves only. Thus the perfect circular polarization is not essential for a possible experimental observation of nonspreading wave packets.

Interestingly, in the EP case, there appears a possibility of the angular localization in minima of the effective potential Γ with the position of the minima being α dependent (compare Fig. 1). If the creation of localized wave packets in such minima were possible it would allow one to control the shape of the trajectories on which the wave packets propagate by a change of microwave polarization, and not by an additional static field as proposed in [18]. Study of the corresponding wave functions indicates, however, that due to the small resonance island width the localization *along* the ellipse [i.e., in $(J, \hat{\theta})$ space] is not very effective at least in the range of n_0 and F_0 studied by us.

ACKNOWLEDGMENTS

We are grateful to Dominique Delande for numerous discussions and the permission to use his Lanczos diagonalization routines. The support of the KBN under Project No. 2P302B-00915 (K.S. and J.Z.) is acknowledged. Numerical calculations were performed at the Academic Computer Center Cyfronet in Kraków with the help of Grant Nos. KBN/S2000/UJ/067/1998 and KBN/S2000/UJ/068/1998. K. Sacha acknowledges financial support from the Foundation for Polish Science.

APPENDIX

Consider the Floquet Hamiltonian H_F as defined in Eq. (2.2) with the Hamiltonian given by (2.1). For the sake of efficiency of the numerical diagonalization it is convenient to rewrite the Floquet Hamiltonian in the velocity gauge by applying a standard unitary transformation [2,39]

$$H_F = -i \frac{\partial}{\partial t} + \frac{p_x^2 + p_y^2}{2} - \frac{1}{r} + \frac{F}{\omega} [p_x \sin \omega t - p_y \alpha \cos \omega t] + \frac{F^2}{4\omega^2} (\alpha^2 + 1). \quad (\text{A1})$$

Next we turn to scaled semiparabolic coordinates (2.3), which allows us to express the Floquet eigenvalue equation

$$H_F|u_n(t)\rangle = E_n|u_n(t)\rangle \quad (\text{A2})$$

as a generalized eigenvalue problem

$$(\mathcal{A} - E_n \mathcal{B})|u_n(t)\rangle = 0, \quad (\text{A3})$$

where

$$\mathcal{A} = (u^2 + v^2)H_F \quad (\text{A4})$$

and

$$\mathcal{B} = u^2 + v^2,$$

with

$$H_F = \frac{p_u^2 + p_v^2}{2\Lambda^2(u^2 + v^2)} - \frac{2}{\Lambda(u^2 + v^2)} - i\frac{\partial}{\partial t} + \frac{F}{\Lambda\omega(u^2 + v^2)} \\ \times [(up_u - vp_v)\sin \omega t - \alpha(vp_u + up_v)\cos \omega t] \quad (\text{A5})$$

(with the additive ponderomotive term omitted).

Floquet states are periodic in time (with the period $T = 2\pi/\omega$), thus we may expand $|u_n(t)\rangle$ in the Fourier series

$$|u_n(t)\rangle = \sum_{K=-\infty}^{+\infty} e^{-iK\omega t}|u_n^K\rangle. \quad (\text{A6})$$

This allows us to cast Eq. (A3) into the equivalent set of coupled equations

$$\left[\frac{p_u^2 + p_v^2}{2\Lambda^2} - \frac{2}{\Lambda} - K\omega(u^2 + v^2) \right] |u_n^K\rangle + (W_s - W_c)|u_n^{K-1}\rangle \\ - (W_s + W_c)|u_n^{K+1}\rangle = E_n(u^2 + v^2)|u_n^K\rangle \quad (\text{A7})$$

where

$$W_s = i\frac{F}{2\omega\Lambda}(up_u - vp_v), \quad (\text{A8})$$

$$W_c = \alpha\frac{F}{2\omega\Lambda}(vp_u + up_v).$$

All terms in the above equation have the polynomial form in coordinates and momenta. This suggests using the harmonic oscillator basis for an efficient evaluation of matrix elements [39]. The method becomes then analogous to the treatment of the circular polarization case discussed in detail elsewhere [33]. The resulting generalized eigenvalue equation is diagonalized using the Lanczos code, which allows for an extraction of eigenvalues in a selected energy range and the corresponding eigenvectors. For completeness let us mention only that the Floquet Hamiltonian is invariant under the generalized parity transformation, i.e., the parity transformation combined with the translation in time by π/ω . Thus \mathcal{A} and \mathcal{B} matrices may be split into uncoupled matrices that are two times smaller. This makes the numerical calculations more efficient.

-
- [1] J. H. Shirley, Phys. Rev. **138**, B979 (1965).
[2] C. Cohen-Tannoudji, J. Dupont-Roc, and G. Grynberg, *Atom-Photon Interactions: Basic Processes and Applications* (John Wiley and Sons, New York, 1992).
[3] A. J. Lichtenberg and M. A. Leiberman, *Regular and Chaotic Dynamics*, 2nd ed. (Springer, New York, 1992).
[4] G. P. Berman and G. M. Zaslavsky, Phys. Lett. **61A**, 295 (1977).
[5] J. Henkel and M. Holthaus, Phys. Rev. A **45**, 1978 (1992); M. Holthaus, Chaos Solitons Fractals **5**, 1143 (1995).
[6] L. Sirko and P. M. Koch, Appl. Phys. B **60**, S195 (1995).
[7] D. Delande and A. Buchleitner, Adv. At., Mol., Opt. Phys. **35**, 85 (1994); A. Buchleitner and D. Delande, Phys. Rev. Lett. **75**, 1487 (1995).
[8] I. Bialynicki-Birula, M. Kalinski, and J. H. Eberly, Phys. Rev. Lett. **73**, 1777 (1994).
[9] D. Delande, J. Zakrzewski, and A. Buchleitner, Europhys. Lett. **32**, 107 (1995).
[10] J. Zakrzewski, D. Delande, and A. Buchleitner, Phys. Rev. Lett. **75**, 4015 (1995).
[11] D. Farrelly, E. Lee, and T. Uzer, Phys. Rev. Lett. **75**, 972 (1995).
[12] I. Bialynicki-Birula, M. Kalinski, and J. H. Eberly, Phys. Rev. Lett. **75**, 973 (1995).
[13] D. Farrelly, E. Lee, and T. Uzer, Phys. Lett. A **204**, 359 (1995).
[14] A. Brunello, T. Uzer, and D. Farrelly, Phys. Rev. Lett. **76**, 2874 (1996).
[15] E. Lee, A. F. Brunello, and D. Farrelly, Phys. Rev. A **55**, 2203 (1997).
[16] C. Cerjan, E. Lee, D. Farrelly, and T. Uzer, Phys. Rev. A **55**, 2222 (1997).
[17] M. Kalinski, J. H. Eberly, and I. Bialynicki-Birula, Phys. Rev. A **52**, 2460 (1995).
[18] K. Sacha, J. Zakrzewski, and D. Delande, Eur. Phys. J. D **1**, 231 (1998).
[19] J. Zakrzewski, D. Delande, and A. Buchleitner, Phys. Rev. E **57**, 1458 (1998).
[20] J. Zakrzewski, D. Delande, and A. Buchleitner, Acta Phys. Pol. A **93**, 179 (1998).
[21] D. Delande and J. Zakrzewski, Phys. Rev. A **58**, 466 (1998).
[22] R. G. Hulet and D. Kleppner, Phys. Rev. Lett. **51**, 1430 (1983).
[23] D. Delande and J. C. Gay, Europhys. Lett. **5**, 303 (1988).
[24] J. Zakrzewski and D. Delande, J. Phys. B **30**, L87 (1997).
[25] K. Hornberger and A. Buchleitner, Europhys. Lett. **41**, 383 (1998).
[26] Z. Bialynicka-Birula and I. Bialynicki-Birula, Phys. Rev. A **56**, 3623 (1997).
[27] A. Buchleitner, D. Delande, and J. Zakrzewski, in *Proceedings of the 7th International Conference on Multiphoton Processes*, edited by P. Lambropoulos and H. Walther (Institute of Physics Publishing, Bristol, 1997).

- [28] A. Buchleitner, K. Sacha, D. Delande, and J. Zakrzewski (unpublished).
- [29] M. R. W. Bellermann, P. M. Koch, D. R. Mariani, and D. Richards, *Phys. Rev. Lett.* **76**, 892 (1996).
- [30] M. Nauenberg, *Europhys. Lett.* **13**, 611 (1990).
- [31] J. E. Howard, *Phys. Rev. A* **46**, 364 (1992).
- [32] J. Zakrzewski, D. Delande, J. C. Gay, and K. Rzążewski, *Phys. Rev. A* **47**, R2468 (1993).
- [33] J. Zakrzewski, R. Gębarowski, and D. Delande, *Phys. Rev. A* **54**, 691 (1996).
- [34] R. V. Jensen, S. M. Susskind, and M. M. Sanders, *Phys. Rep.* **201**, 1 (1991).
- [35] P. M. Koch and K. A. H. van Leeuwen, *Phys. Rep.* **255**, 289 (1995).
- [36] K. Sacha and J. Zakrzewski, *Phys. Rev. A* **56**, 719 (1997).
- [37] K. Sacha and J. Zakrzewski, *Phys. Rev. A* **58**, 488 (1998).
- [38] H. P. Breuer and M. Holthaus, *Ann. Phys. (N.Y.)* **211**, 249 (1991).
- [39] K. Sacha, Ph.D. dissertation, Jagiellonian University, Cracow, Poland, 1998 (unpublished).
- [40] M. Kalinski and J. H. Eberly, *Phys. Rev. A* **53**, 1715 (1996).
- [41] J. G. Leopold and D. Richards, *J. Phys. B* **19**, 1125 (1986).
- [42] I. C. Percival, *Proc. R. Soc. London, Ser. A* **353**, 289 (1977).
- [43] M. Kalinski and J. H. Eberly, *Phys. Rev. A* **52**, 4285 (1995).
- [44] D. Delande, J. Zakrzewski, and A. Buchleitner, *Phys. Rev. Lett.* **79**, 3541 (1997).
- [45] A. Buchleitner, B. Grémaud, and D. Delande, *J. Phys. B* **27**, 2663 (1994).